

Abstract

Using the wavelet technology method and lidar measurements the atmospheric boundary layer height was derived above the city of Lanzhou (China) and its suburb rural area – Yuzhong. Furthermore, at Yuzhong, the average boundary layer height and entrainment zone thickness was derived in convective situations. Simultaneously the boundary layer height was derived from the microwave observations using a profiling radiometer and the parcel method. The results show that both data sets agree in strong convective situations. However, for weak convective situations the lidar measurements reveal boundary layer heights that are higher compared to the microwave observations, because a decrease of the thermal boundary layer height does not directly lead to a drop of aerosols in that altitude layer. Finally, the entrainment zone thicknesses are compared with theoretical predictions, and the results show some consistence between both data sets.

1 Introduction

The boundary layer height (BLH) is a key parameter in describing the structure of the atmospheric boundary layer (BL), it determines the volume available for pollutant dispersion. Currently, the BLH cannot be measured directly and it must be estimated from remote sensing profile measurements. The lidar remote sensing instrument is a useful tool to measure properties of the BL and the BLH.

Lidar backscattering measurements represent the relative concentration profiles of atmospheric aerosols. Generally, most aerosols have their sources at the surface, producing high concentrations in the BL relative to the free atmosphere. There are usually sharp gradients in aerosol concentration at the BL top, this provides a method to determine the BLH.

Early lidar studies of BL used subjective visual estimates to determine the BLH, automated approaches have included the use of simple signal threshold values (Boers

AMTD

5, 1233–1251, 2012

Lidar measurement of planetary boundary layer height

Z. Wang et al.

Title Page

Abstract

Introduction

Conclusions

References

Tables

Figures

⏪

⏩

◀

▶

Back

Close

Full Screen / Esc

Printer-friendly Version

Interactive Discussion



Lidar measurement of planetary boundary layer height

Z. Wang et al.

Title Page	
Abstract	Introduction
Conclusions	References
Tables	Figures
⏪	⏩
◀	▶
Back	Close
Full Screen / Esc	
Printer-friendly Version	
Interactive Discussion	

and Eloranta, 1985), and identifications of the minimum in the vertical gradients of lidar profiles (Flamant et al., 1997) and maximum in variances of lidar signals (Hooper and Eloranta, 1986; Lammert and Boesenberg, 2006). The first of these suffer from the need to define appropriate threshold values, the second approach, the gradient one suffers from the effects of noise and small-scale structure in the lidar profiles. Averaging of the backscatter signal can minimize this problem but inevitably degrades the signal of interest. Steyn et al. (1999) presented an approach that fit an idealized profile to the observed one, another one widely used is based on the continuous wavelet transform method (Cohn and Angevineet, 2000; Davis et al., 2000; Brooks, 2003; Morille et al., 2007). When the vertical distribution of aerosols in the BL consists of a multi-layer structure the lidar determination of the BLH will be complicated because it is not easy to determine a true BL top from these aerosols layer tops. The method applied in this article is based on the work of Morille et al. (2007). It differs from it in two aspects: (i) the multi-layer distribution of the aerosols is retrieved directly instead of single layer; (ii) a set of criterions is proposed to determine BLH from the evolution of multi-layer structure, in which the continuity in evolution of BLH along time is a main consideration.

The entrainment zone thickness is also an important parameter of the BL. An entrainment zone locates at the top of the BL and consists of a mixture of air with the BL and free-troposphere characteristics. It is defined as the region with negative buoyancy flux, however various alternative definitions occur in measurements because of different means (Boers et al., 1986; Nelson et al., 1989; Flamant et al., 1997; Cohn and Angevineet, 2000; Grabon et al., 2010). In this paper the method to find the locations of percentiles of BLH is applied, and the results are compared with that from theoretical models.

In the following, Sect. 2 introduces the sites and data, the method is described in Sect. 3 and results are showed in Sect. 4, Sect. 5 presents the summary and discussion.



2 Observation sites and instrumentation

The data used in this paper are from the Semi-Arid Climate Observatory and Laboratory of Lanzhou University (SACOL) including two sites located at the suburb rural area of Lanzhou – Yuzhong (SACOL-Main) and the city of Lanzhou (SACOL-Lanzhou), respectively. At the city of Lanzhou a micro-pulse lidar (CE370-2) measures the aerosols vertical profiles from ground to 30 km height with a time resolution of 30 min range resolution of 15 m. At Yuzhong, a microwave profiling radiometer (TP/WVP-3000) can obtain the vertical profiles of temperature, water vapor, and liquid water up to 10 km with a time resolution of 1 min and range resolution of 0.1 km for the height below 1 km and 0.25 km for 1–10 km. The fluxes of momentum, latent and sensible heat are measured with a three-axis sonic anemometer (CSAT3) pointed into the prevailing wind direction, a micro-pulse lidar (MPL-4) records backscatter signals up to 20 km with a time resolution of 1 min and range resolution of 75 m.

3 Methodology

3.1 The detection of the BLH

The BLH is determined according to the sharp gradient of lidar profile at the top of the BL, however, the sharp gradient also occurs at the top of cloud or advected aerosols layer, which therefore should be identified firstly. The continuous wavelet transform (CWT) for each lidar profile is computed as

$$\text{CWT}_i(a, b) = \int_{z_1}^{z_2} p(z, t) g_i \left(\frac{z-b}{a} \right) \frac{1}{\sqrt{a}} dz, \quad i = 1, 2 \quad (1)$$

$$g_1(t) = (1 - t^2) e^{-t^2/2} / \sqrt{2\pi} \quad (2)$$

$$g_2(t) = -t e^{-t^2/2} / \sqrt{2\pi} \quad (3)$$

Lidar measurement of planetary boundary layer height

Z. Wang et al.

Title Page

Abstract

Introduction

Conclusions

References

Tables

Figures

⏪

⏩

◀

▶

Back

Close

Full Screen / Esc

Printer-friendly Version

Interactive Discussion



Lidar measurement of planetary boundary layer height

Z. Wang et al.

Title Page

Abstract

Introduction

Conclusions

References

Tables

Figures

⏪

⏩

◀

▶

Back

Close

Full Screen / Esc

Printer-friendly Version

Interactive Discussion



where, $p(z, t)$ represents the range-corrected backscatter. $CWT_1(a, b)$ has its minimum at the top and base of cloud or advected aerosols layer and maximum at their peaks. After determining some possible particles layers, a threshold value $thre1$ is applied. These satisfying $\Delta p = p(z_{peak}, t) - p(z_{base}, t) > thre1$ are considered to be true.

5 Similarly, $CWT_2(a, b)$ has its maximum at the part of lidar profile where the range-corrected backscatter decreases with height. The largest maximum of $CWT_2(a, b)$ often occurs at the top of the BL when both cloud and advected aerosols layer are absent. Currently the following method is applied to retrieve the BLH.

– The first, second and third largest values ($H1, H2, H3$) are selected from the
10 maximums of $CWT_2(a, b)$ except for ones corresponding to the top of cloud or advected aerosols layer. In cloudy situations, only these maximums with locating under the base of the cloud are considered. The locations of the three maximums denote likely BL top.

– $oldblh$ is defined as the average of five successive BLHs with their time before
15 present lidar profile's and the variation of each of them relative to the earlier one all smaller than a threshold $thre2$.

Then, following rules are applied.

1. In cloudless situations, if there is an advected aerosols layer and all maximums
20 of $CWT_2(a, b)$ locating under the base of this aerosol layer are smaller than a threshold $thre3$, then the one closer to the $oldblh$ between its top and base will be considered as the BL top.
2. If (1) dose not match, there is cloud or advected aerosols layer and $H1$ is smaller than a threshold $thre4$, then the base of this cloud or aerosols layer will be considered as the BL top.

Lidar measurement of planetary boundary layer height

Z. Wang et al.

Title Page

Abstract

Introduction

Conclusions

References

Tables

Figures

◀

▶

◀

▶

Back

Close

Full Screen / Esc

Printer-friendly Version

Interactive Discussion

3. If both (1) and (2) do not match, there is neither cloud nor advected aerosols layer and $H1$ is smaller than $thre4$, then the earlier BLH will be considered as a present one.

4. If (1), (2) and (3) do not match, the following functions will be applied,

$$r(x) = \min\left(e^{-\frac{x-c(t)}{\sigma}}, 1\right) \quad (4)$$

$$\text{ratio} = H/H1 \quad (5)$$

where, $c(t) = \min\left(\frac{A_1-A_2}{A_3}t + A_2, A_1\right)$ represents a range in which the difference between two successive BLHs seems reasonable and $\sigma = c(t)/5 \ln 2$. A_1 , A_2 and A_3 are some empirical parameters and t represents time. H represents a one whose height is closer to oldblh between $H2$ and $H3$. $r(|z_{H1} - \text{oldblh}|)$ characterizes a degree to which the height of the $H1$ denotes the true BLH and ratio characterizes a reverse one. If ratio is larger than $r(|z_{H1} - \text{oldblh}|)$, then the location of H will be considered as the BL top, otherwise the location of $H1$ is accepted. This criterion guarantees the temporal continuity of development of the BLH. The parameters in the expressions above vary according to the time resolution of lidar data, the larger the interval between two successive records is, the less important it is.

3.2 Average BLH and entrainment zone thickness

A single lidar profile from MPL-4 represents an average for one minute measurements and the BLH from the single profile denotes local BLH, so average BLH and entrainment zone thickness can be derived from its time sequence. Firstly, calculate a cumulative probability distribution (CPD) of occurrence of the values of the sequence of the BLH for 1 h whose trend has been removed by fitting a second-order polynomial. Then the base and top of the entrainment zone, the average BLH can be defined as the sum

of the value corresponding to 10%, 90% and 50% of CPD and that of the second-order polynomial. At the same time, the BLH is also obtained from temperature profile of TP/WVP-3000 by parcel method (Holzworth, 1964).

3.3 Parameterization theory of entrainment zone thickness

5 According to parcel theory the entrainment zone thickness is related to the kinetic energy and resistance of the air parcel rising (Bores and Eloranta, 1986), and can be written as: $\Delta h \propto \frac{w^2}{g\Delta\theta/\theta_0}$, where Δh is the entrainment zone thickness, g is the gravitational constant, $\Delta\theta$ is the potential temperature jump across the entrainment zone, θ_0 is the average potential temperature in the BL, w is the vertical velocity usually characterized
 10 by the convective velocity scale defined as: $w_*^3 = \frac{g(w'\theta')_s h}{\theta_0}$, where h is the average BLH, $(w'\theta')_s$ is the kinematic heat flux at the surface. Gryning et al. (1994) derived another parameterization theory based on the turbulent-kinetic-energy equation. It can be written as: $\frac{\Delta h}{h} \propto (\text{Ri}_E)^{-1/3}$, where $\text{Ri}_E = \frac{(g/\theta_0)h\Delta\theta}{w_e^2}$ is the entrainment Richardson number, $w_e = \frac{\partial h}{\partial t} - w_L$ is the entrainment velocity, w_L is large-scale mean vertical velocity, which
 15 can be neglected in case of strong convection. In addition, $\frac{\Delta h}{h} \propto \left(\frac{w_e}{w_*}\right)^\alpha$ was proposed by Nelson et al. (1989), where three possible exponents 1.0, 0.5 and 0.25 are suggested. The retrieved entrainment zone thickness is examined through these theories, the kinematic heat flux at the surface is provided by the three-axis sonic anemometer, the mean potential temperature of the BL and potential temperature jump are derived
 20 from temperature profile by the microwave profiling radiometer. However, there may be relatively large errors in the temperature profile due to the limited vertical resolution of the profile data of the profiling radiometer.

Lidar measurement of planetary boundary layer height

Z. Wang et al.

Title Page

Abstract

Introduction

Conclusions

References

Tables

Figures

⏪

⏩

◀

▶

Back

Close

Full Screen / Esc

Printer-friendly Version

Interactive Discussion



4 Results

4.1 Meteorological conditions on Lanzhou

- 28 January 2007: clear sky throughout the whole day.
- 7 January 2007: cirrus coverage of 90 % from 08:00 CST to 17:00 CST, fair weather during the rest of the day.
- 6 July 2008: clear sky throughout the whole day.
- 10 June 2008: almost clear throughout the whole day.

4.2 The BL in the city of Lanzhou

Figures 1 and 2 show lidar observations performed in the city of Lanzhou. Lanzhou is located in a valley basin. The basin is elliptical, surrounded by mountains with the Yellow River flowing across the city. The geography makes it difficult for pollutants to diffuse. The vertical distributions of aerosols in the BL usually show a complicated multi-layer structure. Figure 1 shows the evolution of the heights of H_1 , H_2 and H_3 to illustrate this distinguishing feature. On 28 January 2007, only H_2 and H_3 larger than $0.15 H_1$ have been showed, and $0.25 H_1$ on 7 January 2007.

On 28 January 2007, the aerosols concentrations for the whole day below 0.5 km are relatively high compared to the ones above 0.5 km. There are very strong gradients in aerosols concentration at the top of the aerosols layer, and H_1 mainly denotes its top. After 09:00, the thermal rising of the air-masses produce another aerosol layer with weak gradients at its top above the first one, H_2 denotes its top before 16:00. On 10 June 2008, from 08:00 to 12:00, there are clouds at height of 3.0 km initially, which dissipated and appeared again later. The retrieved BLH when cloudless denotes location of vapor from clouds, and true BLH are denoted by H_2 or H_3 at the height of about 2.0 km.

Lidar measurement of planetary boundary layer height

Z. Wang et al.

Title Page

Abstract

Introduction

Conclusions

References

Tables

Figures

⏪

⏩

◀

▶

Back

Close

Full Screen / Esc

Printer-friendly Version

Interactive Discussion



It is difficult to determine the correct BLH in most cases owing to the multi-layer distributions of aerosols in the city of Lanzhou, so it seems more advisable that the heights of H_1 , H_2 and H_3 are give together, as in Fig. 1.

4.3 The BL in suburb rural area of Lanzhou – Yuzhong

Figure 3 shows the results from lidar and microwave profiling radiometer measurements on 29 July 2007 at SACOL. Between 11:00 and 16:00 the BLH from lidar are about 0.5 km smaller than the ones from microwave profiling radiometer and the latter begin to rise rapidly from 11:00 while the results from the lidar increase more slowly. After 16:00, the BLH retrieved by the parcel method reduce quickly and disappear at 20:00, but results from lidar maintain at heights of 2.0 km. This discrepancy is caused by the fact that the BLH retrieved by the parcel method represents an up limit height that the rising thermal air-masses can reach while that from lidar observation represents the height of the aerosols layer, aerosols do not drop immediately even if the up limit height decreases.

Figure 4 shows results for six measurement days in the period of June to December 2007. In situations with strong convection, the BLH from lidar agrees with that from profiling radiometer measurements, such as the examples in June, July and August show. However, in situations with weak convection, the BLH from lidar is markedly higher, as shown by the observations in September, November and December.

4.4 Examination of entrainment zone thickness by parameterization theory

The method applied in this study to retrieve the entrainment zone thickness is likely suitable for situations with strong convection, so the data from lidar at SACOL on 14, 16, 22, 23 and 29 July 2007 are used and for each day only results from 10:00 to 18:00 are utilized. Figure 5 presents the evolution of the BL on 22 and 23 July 2007.

Lidar measurement of planetary boundary layer height

Z. Wang et al.

Title Page

Abstract

Introduction

Conclusions

References

Tables

Figures

⏪

⏩

◀

▶

Back

Close

Full Screen / Esc

Printer-friendly Version

Interactive Discussion



Lidar measurement of planetary boundary layer height

Z. Wang et al.

Title Page

Abstract

Introduction

Conclusions

References

Tables

Figures

⏪

⏩

◀

▶

Back

Close

Full Screen / Esc

Printer-friendly Version

Interactive Discussion



In Fig. 6 the expression fitted according to the parcel theory is $\Delta h = 0.0065 \left(\frac{w_*^2}{g\Delta\theta/\theta_0} \right)^{0.96}$, the correlation coefficient is $R^2 = 0.59$ using 74 data points. The result following Bores et al. (1986) is $\Delta h = 38.41 \left(\frac{w_*^2}{g\Delta\theta/\theta_0} \right)^{0.41}$. The expression based on the theory proposed by Gryning et al. (1994) is $\frac{\Delta h}{h} = 3.38 (\text{Ri}_E)^{-0.27}$, here correlation coefficient $R^2 = 0.56$ using 62 data points. The result derived by Gryning et al. (1994) is $\frac{\Delta h}{h} = 3.3 (\text{Ri}_E)^{-1/3} + 0.2$. The last fitted relation is $\frac{\Delta h}{h} = 1.8 \left(\frac{w_e}{w_*} \right)^{0.62}$, where the correlation coefficient is $R^2 = 0.49$ for 62 data points.

5 Conclusions

The BLH over the city of Lanzhou and its suburb rural area – Yuzhong has been obtained using a modified wavelet technology and lidar data. The results reveal the effectiveness of this method. At Yuzhong, the BLH is also calculated using data of microwave profiling radiometer. The comparison shows that both data sets agree under strong convective conditions when the BL grows. However, under conditions with weak convection the lidar data reveal higher values for the BLH. Further, in the case of Yuzhong the entrainment zone thickness is derived from the BLH. The comparison between measured quantity and that predicted by several theories reveals that some consistence exists in them but the difference is also obvious.

Some characteristics about the BL can be concluded from these results. The BLH above the city of Lanzhou often maintains at about 0.5 km throughout the whole day without significant development in winter. At Yuzong, the largest height the BL can reach up to 2.0 km throughout the day in summer and about 1.0 km in winter. Of course, the above-mentioned values are not representative in the statistical sense.

Lidar measurement of planetary boundary layer height

Z. Wang et al.

Title Page

Abstract

Introduction

Conclusions

References

Tables

Figures

⏪

⏩

◀

▶

Back

Close

Full Screen / Esc

Printer-friendly Version

Interactive Discussion



An ideal condition for a lidar to retrieve the BLH is that the lower atmosphere can be divided into three parts according to the aerosols distribution, the BL with much aerosols and tiny variation in aerosols concentration, the entrainment zone with pronounced drop in aerosols concentration and free atmosphere with little aerosols. So the BLH from the lidar represents a surface-based aerosol layer's depth and does not necessarily agree with the one defined by thermodynamics and dynamic properties of the BL.

Clouds have a great impact on the results of the BLH derived by the lidar. For the nascent clouds with strong gradients in the lidar signals at their tops, but without affirmed cloud characteristics, the above-mentioned algorithm likely reveals their tops as those of the BL. Sometimes the lidar profiles will be disorderly preventing the retrieval of useful information when boundary layer clouds are dissipating. Moreover, false BLH maybe appear owing to the remanent vapors.

Convection boundary layer begins to grow after sunrise, however, it is difficult for a lidar to capture its top before it grows beyond the nocturnal boundary layer.

Acknowledgements. The research is supported by the National Important Science Research Program of China (2012CB955302) and the National Natural Science Foundation of China (41075104). We gratefully thank the Semi-Arid Climate Observatory and Laboratory of Lanzhou University providing observation data.

References

- Baars, H., Ansmann, A., Engelmann, R., and Althausen, D.: Continuous monitoring of the boundary-layer top with lidar, *Atmos. Chem. Phys.*, 8, 7281–7296, doi:10.5194/acp-8-7281-2008, 2008.
- Boers, R. and Eloranta, E. W.: Lidar measurements of the atmospheric entrainment zone and the potential temperature jump across the top of the mixed layer, *Bound.-Lay. Meteorol.*, 34, 357–375, 1986.
- Brooks, I.: Finding boundary layer top: application of a wavelet covariance transform to lidar backscatter profiles, *J. Atmos. Ocean Tech.*, 20, 1092–1105, 2003.

Lidar measurement of planetary boundary layer height

Z. Wang et al.

[Title Page](#)[Abstract](#)[Introduction](#)[Conclusions](#)[References](#)[Tables](#)[Figures](#)[⏪](#)[⏩](#)[◀](#)[▶](#)[Back](#)[Close](#)[Full Screen / Esc](#)[Printer-friendly Version](#)[Interactive Discussion](#)

- Cohn, S. A. and Angevine, W. M.: Boundary layer height and entrainment zone thickness measured by lidars and wind-profiling radars, *J. Appl. Meteorol.*, 39, 1233–1247, 2000.
- Davis, K. J., Gamage, N., Hagelberg, C. R., Kiemle, C., Lenschow, D. H., and Sullivan, P. P.: An objective method for deriving atmospheric structure from airborne lidar observations, *J. Atmos. Ocean Tech.*, 17, 1455–1468, 2000.
- De Haij, M., Wauben, W., and Bltink, H. K.: Determination of mixing layer height from ceilometer backscatter profiles, Royal Netherlands Meteorological Institute, P.O. Box 201, 3730 AE De Bilt, The Netherlands.
- Emeis, S. and Schafer, K.: Remote sensing methods to investigate boundary-layer structures relevant to air pollution in cities, *Bound.-Lay. Meteorol.*, 121, 377–385, 2006.
- Emeis, S., Muenkel, C., Vogt, S., Mueller W. J., and Schaefer, K.: Atmospheric boundary-layer structure from simultaneous SODAR, RASS, and ceilometer measurements, *Atmos. Environ.*, 38, 273–286, 2004.
- Emeis, S., Schaefer, K., and Muenkel, C.: Surface-based remote sensing of the mixing-layer height – a review, *Meteorol. Z.*, 17, 621–630, 2008a.
- Emeis, S., Schafer, K., and Munkel, C.: Long-term observations of the urban mixing-layer height with ceilometers, 14th international symposium for the advancement of boundary layer remote sensing, 2008b.
- Flamant, C., Pelon, J., Flamant, P. H., and Durand, P.: Lidar determination of the entrainment zone thickness at the top of the unstable marine atmospheric boundary layer, *Bound.-Lay. Meteorol.*, 83, 247–284, 1997.
- Grabon, J. S., Davis, K. J., Kiemle, C., and Ehret, G.: Airborne lidar observations of the transition zone between the convective boundary layer and free atmosphere during the international H₂O project (IHOP) in 2002, *Bound.-Lay. Meteorol.*, 134, 61–83, 2010.
- Gryning, S. E. and Batchvarova, E.: Parameterization of the depth of the entrainment zone above the daytime mixed layer, *Q. J. Roy. Meteor. Soc.*, 120, 47–58, 1994.
- Holzworth, C. G.: Estimates of mean maximum mixing depths in the contiguous United states, *Mon. Weather Rev.*, 92, 235–242, 1964.
- Hooper, W. P. and Eloranta, E.: Lidar measurements of wind in the planetary boundary layer: the method, accuracy and results from joint measurements with radiosonde and kytoon, *J. Clim. Appl. Meteorol.*, 25, 990–1001, 1986.
- Lammert, A. and Boesenberg, J.: Determination of the convective boundary-layer height with laser remote sensing, *Bound.-Lay. Meteorol.*, 119, 159–170, 2006.

Lidar measurement of planetary boundary layer height

Z. Wang et al.

- Morille, Y., Haefelin, M., Drobinski, P., and Pelon, J.: STRAT: an automated algorithm to retrieve the vertical structure of the atmosphere from single-channel lidar data, *J. Atmos. Ocean. Tech.*, 24, 761–775, 2007.
- 5 Nelson, E., Stull, R. B., and Eloranta, E.: A prognostic relation for entrainment zone thickness, *J. Appl. Meteorol.*, 28, 885–903, 1989.
- Seibert, P., Beyrich, F., Gryning, S.-E., Sylvain, J., Rasmussen, A., and Tercier, P.: Review and intercomparison of operational methods for the determination of the mixing height, *Atmos. Environ.*, 34, 1001–1027, 2000.
- 10 Steyn, D., Baldi, M., and Hoff, R. M.: The detection of mixed layer depth and entrainment zone thickness from lidar backscatter profiles, *J. Atmos. Ocean. Tech.*, 16, 953–959, 1999.
- Stull, R. B.: *An Introduction to boundary Layer Meteorology*, Kluwer Academic Publishers, Dordrecht/Boston/London, 1988.
- Wilde, N. P., Stull, R. B., and Eloranta, E. W.: The LCL zone and cumulus onset, *J. Clim. Appl. Meteorol.*, 24, 640–657, 1985.

Title Page

Abstract

Introduction

Conclusions

References

Tables

Figures

◀

▶

◀

▶

Back

Close

Full Screen / Esc

Printer-friendly Version

Interactive Discussion

Lidar measurement of planetary boundary layer height

Z. Wang et al.

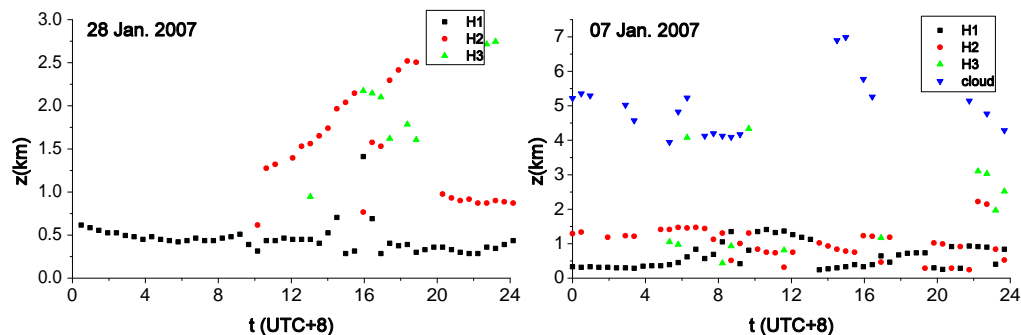


Fig. 1. Evolution of aerosol layer height in winter. Each dot represents the average for five minutes measurements. Measurements were taken every 30 min.

[Title Page](#)[Abstract](#)[Introduction](#)[Conclusions](#)[References](#)[Tables](#)[Figures](#)[⏪](#)[⏩](#)[⏴](#)[⏵](#)[Back](#)[Close](#)[Full Screen / Esc](#)[Printer-friendly Version](#)[Interactive Discussion](#)

Lidar measurement of planetary boundary layer height

Z. Wang et al.

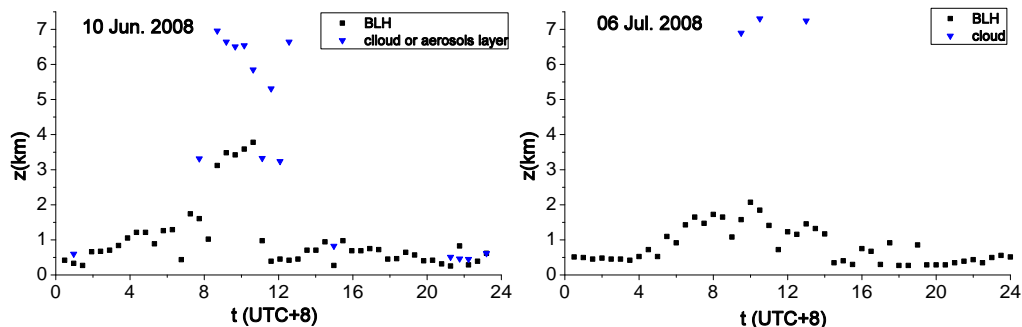


Fig. 2. Evolution of the BLH retrieved from lidar in summer. Each dot represents the average for five minutes measurements. Measurements were taken every 30 min.

[Title Page](#)[Abstract](#)[Introduction](#)[Conclusions](#)[References](#)[Tables](#)[Figures](#)[⏪](#)[⏩](#)[◀](#)[▶](#)[Back](#)[Close](#)[Full Screen / Esc](#)[Printer-friendly Version](#)[Interactive Discussion](#)

Lidar measurement of planetary boundary layer height

Z. Wang et al.

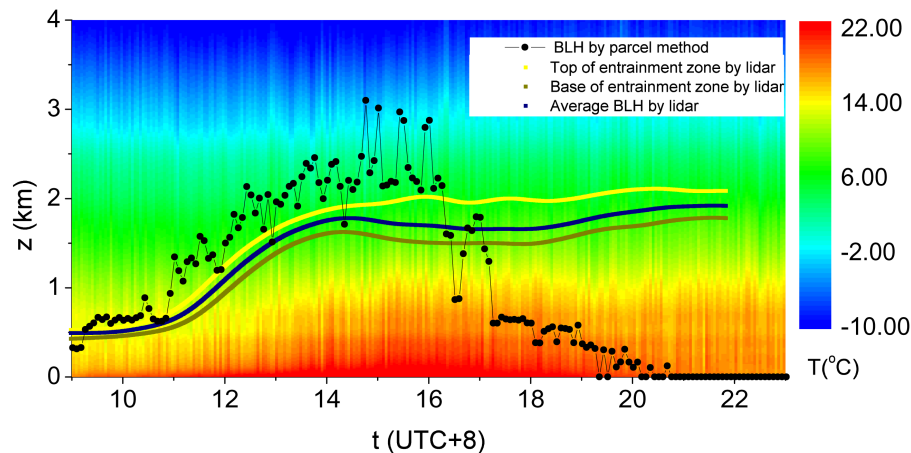


Fig. 3. Comparison between results from lidar and microwave profiling radiometer measurements for 29 July 2007. The dotted line represents the BLH from the microwave profiling radiometer determined by the parcel method and each dot is the average for five minutes measurements.

[Title Page](#)[Abstract](#)[Introduction](#)[Conclusions](#)[References](#)[Tables](#)[Figures](#)[⏪](#)[⏩](#)[◀](#)[▶](#)[Back](#)[Close](#)[Full Screen / Esc](#)[Printer-friendly Version](#)[Interactive Discussion](#)

Lidar measurement of planetary boundary layer height

Z. Wang et al.

Title Page

Abstract

Introduction

Conclusions

References

Tables

Figures

◀

▶

◀

▶

Back

Close

Full Screen / Esc

Printer-friendly Version

Interactive Discussion

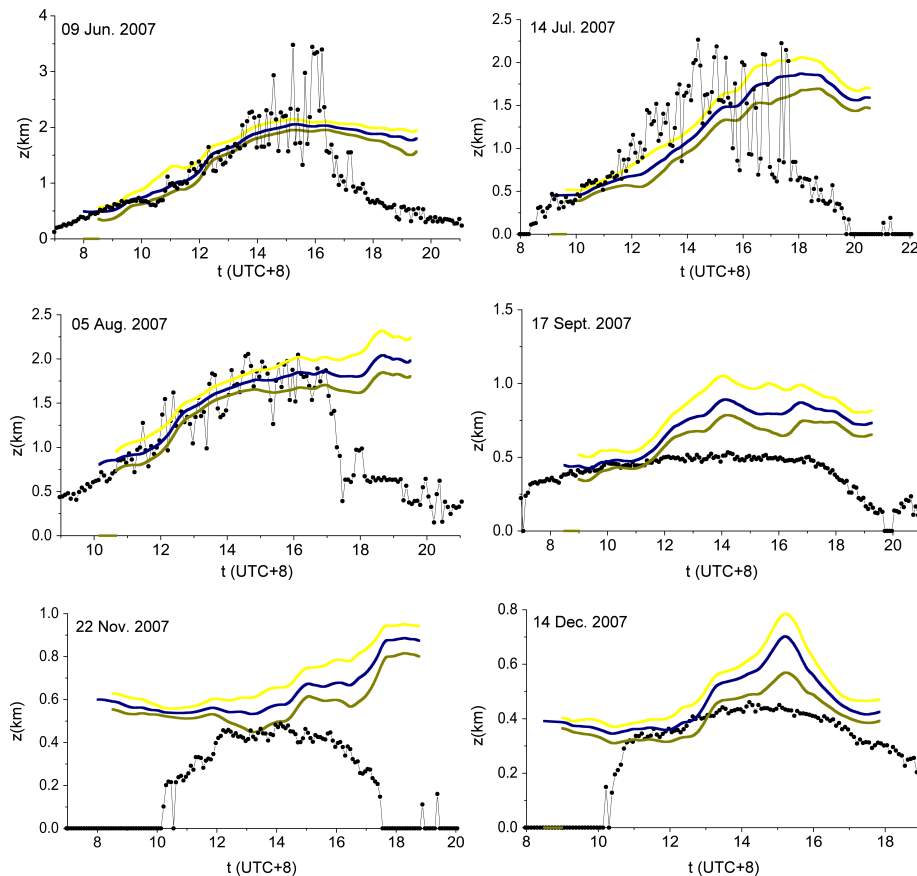


Fig. 4. Comparisons between the BLH from lidar and microwave profiling radiometer for six measurement days in the period of June to December 2007. The contents are the same as Fig. 3 except that temperature measurements are not showed.

Lidar measurement of planetary boundary layer height

Z. Wang et al.

Title Page

Abstract

Introduction

Conclusions

References

Tables

Figures

⏪

⏩

◀

▶

Back

Close

Full Screen / Esc

Printer-friendly Version

Interactive Discussion

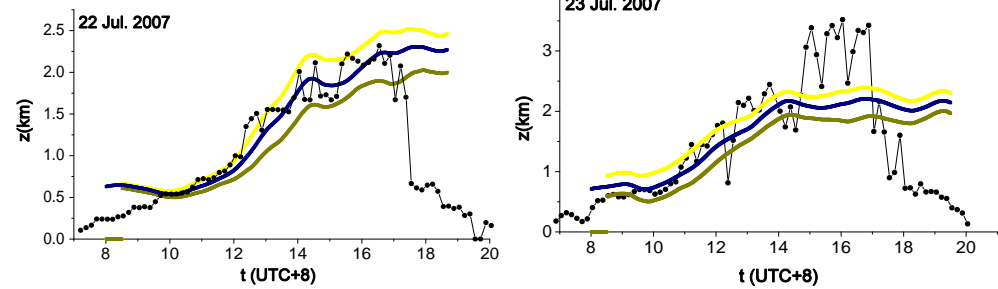


Fig. 5. Same as Fig. 4 except for 22 and 23 July 2007.

Lidar measurement of planetary boundary layer height

Z. Wang et al.

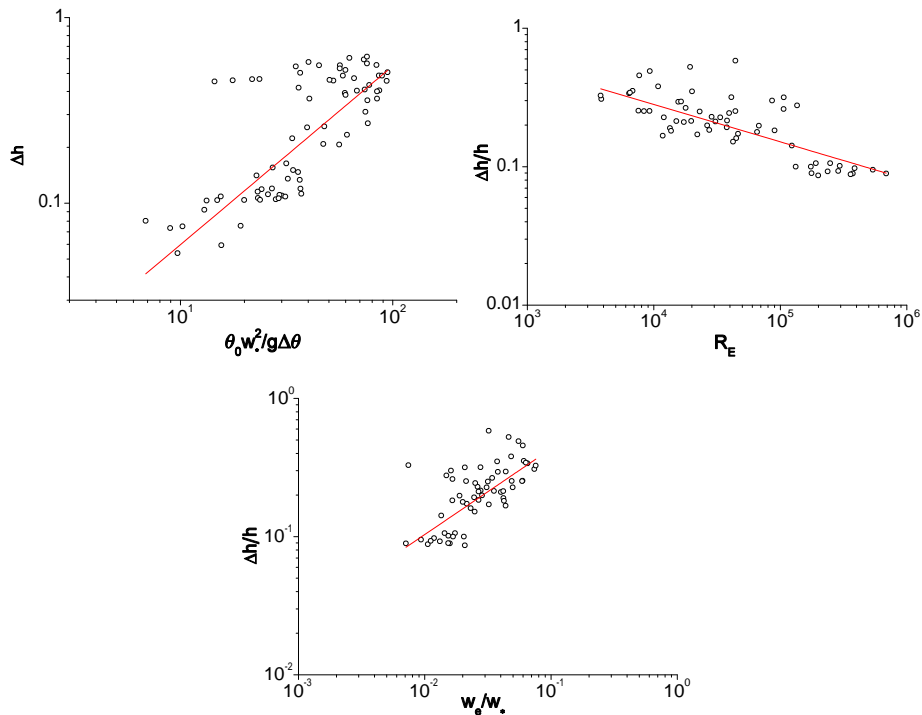


Fig. 6. Comparison between entrainment zone thicknesses from lidar and theoretical prediction.

Title Page

Abstract

Introduction

Conclusions

References

Tables

Figures

◀

▶

◀

▶

Back

Close

Full Screen / Esc

Printer-friendly Version

Interactive Discussion

